



Experimental Study on Stress Transfer and Fracture Law During the Hydraulic Fracturing of Coal Seams

Xiaoguang Wang · Qianting Hu · Quangui Li

Received: 9 September 2020 / Accepted: 14 March 2021 / Published online: 19 March 2021
© The Author(s), under exclusive licence to Springer Nature Switzerland AG 2021

Abstract Hydraulic fracturing is a key technology for increasing the permeability of coal seams and improving the extraction effect of coalbed methane. Exploring the parameters that represent the infiltration effect is an essential part of the optimization process of hydraulic fracturing. In this work, based on a similarity principle design, a hydraulic fracturing test was carried out on large raw coal samples using an indoor hydraulic fracturing physical simulation test system. Based on the distribution of primary cracks in the coal samples, the law of crack extension during hydraulic fracturing was studied. The stress variations before and after hydraulic fracturing of the coal seams were monitored, and the stress transfer laws during confining pressure loading and hydraulic fracturing were

investigated. The experiment showed that the new fissures in the fracturing process are more likely to extend to the primary fissure development area. When the applied coal body stress exceeds the strength of the coal sample body, the internal cracks in the coal sample are completely penetrated. During this complete penetration, the energy accumulated by pressure water injection is continuously released, and the count detected by the acoustic emission increases sharply. The coal is mainly subjected to compressive stress during the confining pressure loading process, whereas the coal body is mainly subjected to a shear stress during the hydraulic fracturing process. Both the stresses can be transferred through the coal samples. When the stress increase during hydraulic fracturing is greater than the confining load, the overall effect is due to different stresses. As the cracks continue to expand and extend during hydraulic fracturing, the stress transfer effect becomes weaker. Through the exploration of the law of crack extension and stress transmission, this experiment showed that large-scale physical simulation experiments in a laboratory setting can help effectively simulate on-site hydraulic fracturing conditions. The test method and results reported herein provide a reference and basis for the design and optimization of on-site hydraulic fracturing parameters.

X. Wang (✉)
State Key Laboratory of Mountain Bridge and Tunnel Engineering, Chongqing Jiaotong University,
Chongqing 400074, China
e-mail: Dwanxg@163.com

X. Wang
School of Civil Engineering, Chongqing Jiaotong University, Chongqing 400074, China

Q. Hu · Q. Li
State Key Laboratory of Coal Mine Disaster Dynamics and Control, Chongqing University, Chongqing 400044, China

Q. Hu · Q. Li
College of Resources and Environmental Science, Chongqing University, Chongqing 400044, China

Keywords Hydraulic fracturing · Similarity design · Stress monitoring · Acoustic emission response

1 Introduction

Physical simulation of fracture propagation during the hydraulic fracturing of coal involves simulating the expansion of coal rock gas wells under specific reservoir conditions. The actual physical process of coal rock hydraulic crack propagation has been scientifically described through direct observation or by determining the morphological parameters related to hydraulic fractures. The physical simulation experiment on crack propagation during hydraulic fracturing in coal rocks is an important method to understand the fracture morphology and crack propagation law, and it is also the main means to verify and improve theoretical and numerical models (Shi et al. 2016).

During the hydraulic fracturing process of coal reservoirs, the shape and expansion law of coal-rock hydraulic fractures are affected by the special structure and physical properties such as the development of their own pore fractures, heterogeneous discontinuity, low elastic modulus and high Poisson's ratio. Many foreign scholars have conducted research on this issue. Bell (1989); Abass (1990) and (1991); Arash Dahi. (2009); M. Khodaverdian et al. (1991) conducted a hydraulic fracturing simulation experiment of medium coal rank coals in shallow reservoirs (200 ~ 400 m). The results show that in the hydraulic fracturing process, a relatively large horizontal crack or vertical crack can be formed under a large principal stress difference. There is a large pressure drop in the cracks near the wellbore due to the development of primary cracks, clogging of coal powder at the entrance to the crack, and pore pressure. Papadopoulos et al. (1983) used hydraulic samples instead of natural rock samples to carry out hydraulic fracturing simulation experiments, and analyzed the multi-crack expansion process and its interaction. Dehghan et al. (2016) confirmed that natural cracks around the wellbore can reduce the effects of the original stress concentration, leading to a sharp decrease in crack initiation and expansion pressure. Teufel et al. (1984) believed that the difference in mechanical properties of layered rock and the shear strength of the boundary surface play a role in controlling the morphology of hydraulic fractures.

Many domestic scholars have done a lot of research on hydraulic fracturing physical similarity simulation experiments. Wong et al. (2002) analyzed the expansion law of prefabricated cracks of different shapes

and orientations in rock specimens under external loads by hydraulic fracturing physics simulation experiments. Wang et al. (2006) used cement mortar samples instead of natural rock samples for hydraulic fracturing experiments, and analyzed the basis for judging the fracture of heterogeneous rocks. Meng et al. (2016) analyzed the effects of the elastic modulus difference, the ground stress difference and the natural weakness on the crack initiation and propagation of hydraulic cracks and the penetration conditions through the indoor large-scale test. Li et al. (2015) studied the influence of formation parameters on hydraulic crack initiation. It is believed that when the pumping pressure remains unchanged, the increase of coal seam porosity, permeability, Poisson's ratio and elastic modulus can cause hydraulic cracks to crack as early as possible. Chen et al. (2000); Jin et al. (1999); Deng et al. (2004); Zhou et al. (2007); Shi et al. (2008) and Lin et al. (2011) carried out a physical simulation experiment of coal fracturing hydraulic fracturing using a large-scale hydraulic fracturing experimental device. The above research plays a role in understanding and understanding the mechanism of hydraulic fracturing crack propagation in coal and rock. The expansion and extension of hydraulic fracturing cracks is generally accompanied by the transmission of coal and rock stress. Exploring the coal seam stress transfer law during hydraulic fracturing is a non-negligible factor. The larger the coal sample size, the more similar the coal sample condition is to the on-site coal seam, and the more accurate the simulation of the on-site hydraulic fracturing experiment. The experimental results obtained in this way have scientific guidance for the actual coal reservoir hydraulic fracturing project.

In this study, a sample with dimensions of 800 mm × 800 mm × 1500 mm was fabricated using a similarity design method. Based on an actual coal reservoir hydraulic fracturing project, a physical simulation experiment scheme for the crack expansion in the coal sample during hydraulic fracturing was developed, and a coal-rock hydraulic pressure experiment and a stress monitoring experiment were carried out under existing experimental conditions. Acoustic emission sensors are arranged based on the distribution of primary fractures in coal samples to monitor the fracture signals of coal samples caused by fracturing. Explore the law of fracture extension during hydraulic fracturing. It is helpful to determine the effective area

of gas drainage after fracturing and improve the gas drainage efficiency. Collect coal seam stress during hydraulic fracturing, and summarize the stress time-space evolution law during hydraulic fracturing. It helps to determine the coal seam mining cycle after fracturing on site and avoid possible coal and gas outburst accidents caused by stress concentration caused by fracturing. Through the analysis of the experimental results, the crack propagation law and coal–rock stress transmission law during hydraulic fracturing were investigated. The research results can provide a reference and basis for the parameter design and optimization of on-site hydraulic fracturing.

2 Experimental Study

2.1 Similarity Experiment Design

2.1.1 Similarity Conditions

The physical simulation experiment involves reconstructing the phenomenon of natural or on-site production using experimental methods to make it partially or completely reproducible. It is used to observe phenomena that cannot be directly observed in natural or on-site production, and to study the variation in the model under conditions of simulating natural or certain on-site factors. The main advantage is that the test can be carried out without considering the many factors influencing the research object. Similarity simulation is an important method for studying specific engineering problems. Through simulation experiments, a similar relationship is established between a model and a prototype to meet the similarity requirements. The similarity theorem provides a theoretical basis for similarity model experiments.

According to certain principles, the parameters are reasonably selected, the secondary elements are ignored, and the main factors are selected, thus realizing simulation research. The similar conditions are determined according to the particularity of the research object. The similarity conditions are the conditions that the relevant parameters of the model and prototype should meet when performing similar simulation tests (as listed in Table 1).

2.1.2 Coal Pore Characteristics

Similar materials are an important part of similar model tests. The correct selection of similar materials is not only decisive for the reliability and accuracy of experimental research but is also key to an appropriate simulation of engineering prototypes. In the similar model test, based on the similarity theory, prototype material, and certain similarity ratio, the similar materials required for the test were obtained through repeated tests of the physical and mechanical properties.

2.1.2.1 Structural Features of Coal Samples

The coal structure can be characterized by the size and shape of the coal particles and is one of the important factors affecting the physical properties of coal seams. In China, the structure of coal is divided into five categories based on the degree of coal damage. The degree of damage to the coal seam is III-V-type damage, which can be broken by handcuffs, and the strength of the coal is low. Therefore, this test is similar to the simulation test, and the uniaxial compressive strength of similar materials is ≤ 1 MPa as the mechanical property evaluation index.

2.1.2.2 Porosity Characteristics and Specific Surface Area of Coal Samples

Coal micropores are relatively developed, and as the type of coal failure increases, the total volume of the pores increases. By testing the pore fracture characteristics of the sampled coal seam, the porosity of the coal sample was found to be 10.79%. The permeability of the coal is related to the ground stress, coal structure, temperature, gas pressure, and moisture. The coal sample structure is complex, the anisotropy is strong, the bedding is more disordered, cracks that form infiltration sites are fewer in number, the penetration resistance is higher, and the permeability is poor. The coal sample permeability value was measured to be $27.08 \times 10^{-9} \mu\text{m}^2$, as shown in Fig. 1. The test coal sample had an f value of 0.3 as confirmed by a laboratory test.

2.1.3 Similar Materials

Selection of cementing materials: Cement was used as the similarity simulation material. Cementing materials are the main raw materials determining the physical and mechanical properties of similar

Table 1 Similarity conditions

Similarity principle	Geometric similarity	Mechanical similarity conditions	Deformation similarity conditions	Destroy similarity conditions
Satisfaction conditions	$l/l' = C_l$	$\delta = \frac{F_s - F_{\min}}{F_{\max} - F_{\min}}$	$\delta F_s F_{\max}$	$F_{\min} C_\phi = 1$

C_l - Geometric similarity constant; l - Prototype geometry feature parameter; l' - Model geometry size parameters. C_σ - Stress similarity constant. ε - No dimension; C_ϵ - Strain similarity constant; C_μ - Poisson’s ratio similarity constant; C_E - Elastic modulus similarity constant. C_c - Cohesion; C_ϕ - Internal friction angle similarity constant.

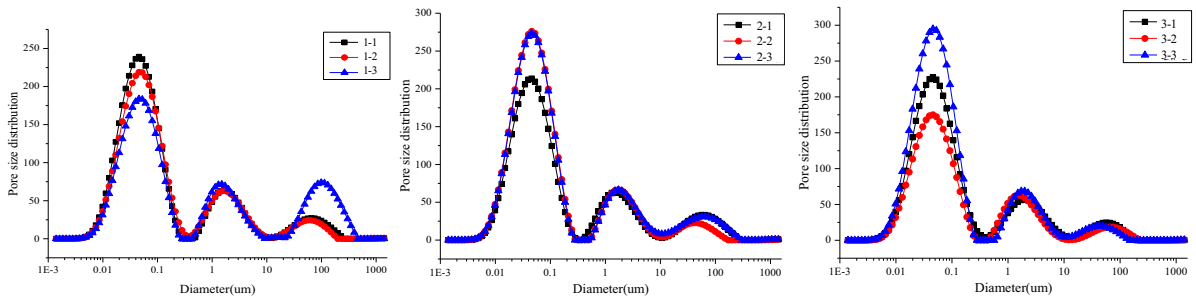


Fig. 1 Coal sample porosity characteristic test

materials. Cementing materials can be used to prepare similar materials with a wide range of strengths and can produce materials with similar compressive and tensile strength ratios. Their brittleness characteristics are consistent with the brittle material characteristics of coal bodies. We used ordinary Portland cement # 425 (Table 2).

Aggregate selection: To ensure that the porosity of the produced briquette is similar to that of the raw coal, and a large amount of pulverized coal is easily obtained, pulverized coal with particles that pass through mesh sizes of 80–40 and 40–20 was selected as the filling material. It was taken from 8# coal seam of Shihao Coal Mine, Chongqing Fuxin Energy Co., Ltd. The 8# coal seam is anthracite, and the coal seam

inclination angle is in the range of 5–11°. The gas content of the coal seam is in the range of 15.08–29.4 m³/t, the gas pressure is in the range of 2.24–4.87 MPa, the permeability coefficient of the coal seam is 21.2 m²/(MPa·d), the type of failure is V, and the initial velocity of gas emission is in the range of 22–43 m³. After being air-dried, it is sieved to obtain two grades of coal samples, ones that pass through 80–40 and 40–20 meshes, for similar material aggregates.

Accessories selection: To match the cement to play the corresponding cementation, water should be selected as the auxiliary material. The aggregate pulverized coal was blended with raw materials such as cement, sand, and water that do not have adsorption characteristics. To maintain the coal briquettes with

Table 2 Physical properties of the tested coal samples

Number	Porosity (%)	Pore size distribution			Average aperture/ μm	Specific surface area/ m ² /g	Permeability/10 ⁻⁹ μm ²
		Big hole/ %	Middle hole/ %	Small hole/ %			
1	26.04	99.95	0.05	0.00	22.20	0.02	36.30
2	10.01	89.36	0.00	10.64	21.98	0.92	23.39
3	10.79	88.08	0.13	11.78	22.35	1.27	27.08

adsorption characteristics similar to those of the raw coal, it is necessary to add the adsorption property of the activated coal to regulate the briquette with better adsorption performance, including sand, activated carbon, and water. Among them, the sand has a particle size of 40 to 20 mesh dry river sand. The activated carbon is in the form of dry granules. The water used was ordinary tap water. Table 3 lists the material distribution. Table 4 lists the basic physical and mechanical parameters of similar coal samples.

2.2 Hydraulic Fracturing Experiment Design

2.2.1 Sample Preparation

The raw coal used for the test was taken from Shihao Coal Mine, Qijiang District, Chongqing (as shown in Fig. 2a). The raw coal was pulverized using a pulverizer, and a coal sample having a particle size of 10–40 mesh was selected using a sieving machine (as shown in Fig. 2b). Based on the parameters listed in Table 1, the coal sample was matched. The proportion of materials mainly include cement, sand, water, and activated carbon (as shown in Fig. 2c). Finally, the coal sample was produced (as shown in Fig. 2d), and the dimensions of the coal sample size were 800 mm × 800 mm × 1500 mm. Since the coal sample size was relatively large and cannot be compacted by one press, a layered pressing was used in the preparation process, and a coal sample of approximately 10 cm in height was placed each time and then compacted using a press.

2.2.2 Test System and Stress Loading

2.2.2.1 Test System The hydraulic fracturing physical similarity test system was built around the coal and gas outburst simulation test system

independently developed by Chongqing Research Institute of China Coal Science and Technology Group. It has large servo pressure loading systems, high-pressure hydraulic fracturing, similar material preparation, acoustic emission monitoring, loading pressure monitoring, and water pressure monitoring.

Fig. 3a shows the two-way hydraulic servo simulation test system used in this study. The main parameters and features are explained as follows: (1) It can be loaded independently in the X and Y directions to realize the simulation loading of the ground stress in the two directions; (2) The maximum load can reach 2500 kN; (3) The sample dimensions are 800 mm × 800 mm × 1500 mm; (4) The load pressure is uniform, and the load force is controlled, thus effectively avoiding the generation of eccentric force and bending moment.

2.2.2.2 Stress Loading The in situ stress measurement points in the Shihao Coal Mine are arranged in a gas tunnel of 60 m from the coal floor, approximately 627 m from the surface. The measurement results of the in situ stress are the maximum horizontal in situ stress $\sigma_1 = 24.3$ MPa, azimuth angle NE117.5°, inclination angle 12°; the minimum horizontal ground stress is $\sigma_3 = 17.8$ MPa, azimuth angle is NE209.3°, and inclination angle is 8.2°; the vertical stress $\sigma_2 = 20.1$ MPa, the azimuth angle is NE332°, and the tilt angle is 75.3°.

The coal seam stress is obtained using hard rock layers in coal-bearing formations to measure the ground stress and is based on a combined spring model. The horizontal deformation of the rock formation due to tectonic action is inversed, and the boundary conditions of the finite element analysis model of the entire coal-bearing formation are applied. Through a finite element simulation, the horizontal in situ stress component due to the horizontal structure

Table 3 Reasonable ratio of similarity simulation materials

Raw material name	Ratio/%	Quality/kg	Remarks
Cement	6.09	104	# 425 Portland cement
Sand	4	68.4	Ordinary dry river sand, grain size 40–20 mesh
Water	5	85.5	Tap water
Activated carbon	2	34.2	Φ2.6×5.6 mm granular and dry
Powder coal	82.91	1417.7	Naturally dry, grain sizes 80–40 and 40–20 meshes, the mass ratio of the two is 1:1.

Table 4 Basic physical parameters of similar simulated materials

Uniaxial compressive strength (MPa)	Robustness factor (f)	Elastic modulus (MPa)	Density (g/cm ³)
1	0.154	63.67	1.34–1.4

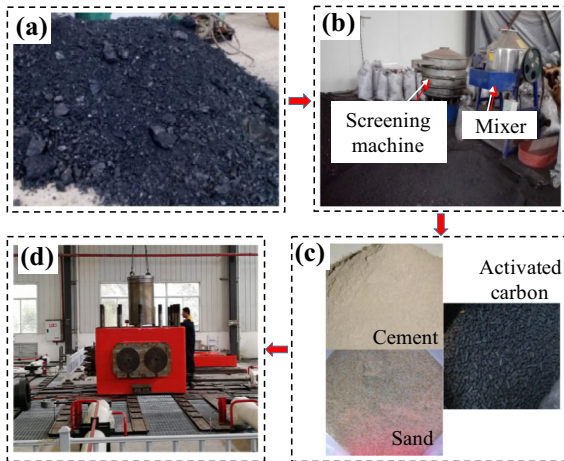


Fig. 2 Coal sample ratio

of the coal seam and that generated by the self-weight of the overburden are obtained, and finally, the horizontal in situ stress of the coal seam is obtained. Table 5 lists the calculation of the coal seam stress results.

Based on the similarity criterion of the similar simulation experiment, the in situ stress condition of the laboratory experiment is the same as the basic model on site. Therefore, the axial and horizontal loads were set to 12 and 10.3 MPa, respectively.

2.2.2.3 Monitoring Means Acoustic emission monitoring systems are widely used in rock material monitoring and other fields. Two indoor acoustic emission probes with an operating frequency range of

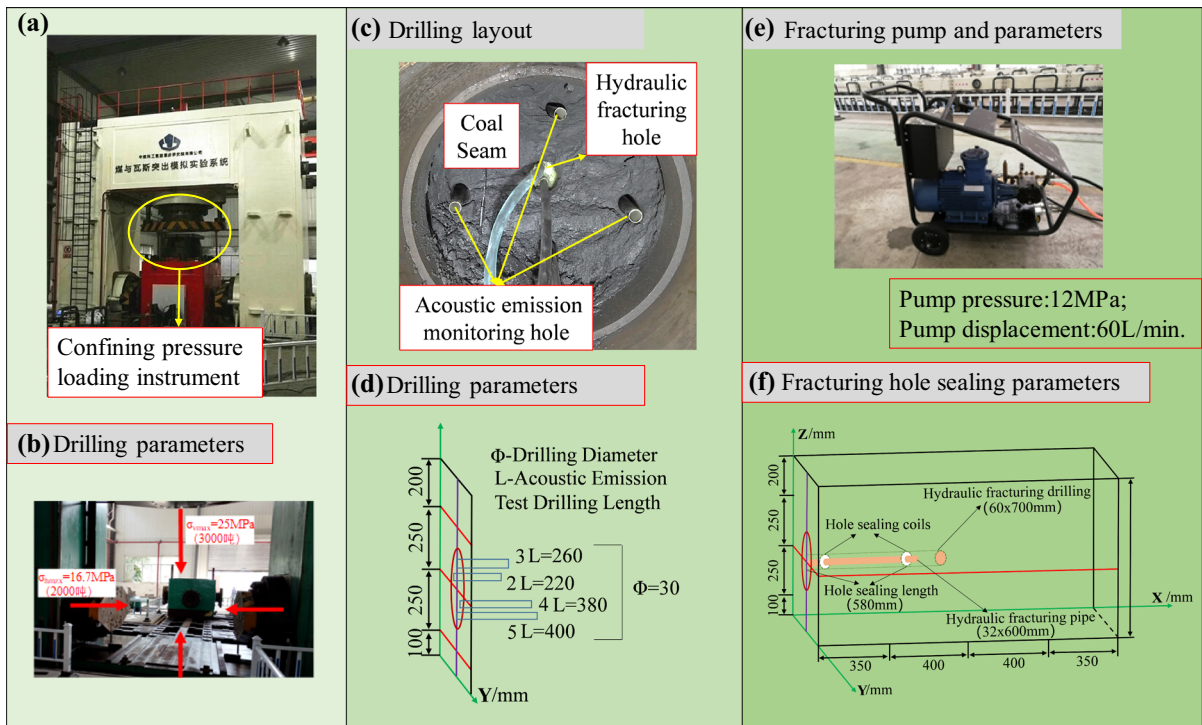


Fig. 3 Experimental scheme of coal seam hydraulic fracturing stress evolution

Table 5 Coal seam stress data sheet

Layer	Main stress	Measured value /MPa	Azimuth /°	Inclination /°
Coal seam	Maximum horizontal stress σ_1	13.48	117.5	12
	Vertical stress σ_2	11.9	332	75.3
	Minimum horizontal stress σ_3	11.8	209.3	8.2

25–70 kHz and a center frequency of 50 kHz were used for the indoor hydraulic fracturing test. To improve the monitoring effect, an acoustic emission probe was placed asymmetrically on each of the two end surfaces of the simulated horizontal in situ stress, and the probe was bonded to the steel pipe using a coupling agent to effectively monitor the crack information.

To meet the requirements of acoustic emission monitoring during hydraulic fracturing, pre-buried steel pipes were drilled at the fracturing port to monitor the acoustic signals more effectively during hydraulic fracturing. Four 25 mm acoustic emission probe monitoring holes were drilled. The position of the probe could be adjusted on the basis of the 3D positioning effect of the acoustic emission to meet the effect of space monitoring. Fig. 3c shows the acoustic emission drilling layout.

The stress variation in the hydraulic fracturing process was explored by arranging stress sensors in different directions and different layers of the same layer of the coal sample. Table 6 lists the sensor parameters; Fig. 4 shows the sensor arrangement.

2.2.3 Fracturing Parameter Design

2.2.3.1 Fracturing Equipment The coal samples were fractured using a high-pressure water pump (Fig. 3e). The maximum loading pressure of the water pump was 150 MPa, the control accuracy was 5%, and the measurement accuracy was 3%. The booster had a volume of 500 mL, and the measurement accuracy was 0.2 mL. The system can be used to simulate

constant-discharge pumping by simulating the actual working conditions. The data collected during the test were mainly water pressure data.

2.2.3.2 Fracturing Drilling Design The diameter and depth of the fracturing holes for this hydraulic fracturing were designed according to a ratio of 1:30. The hole depth, hole diameter, and sealing length were 700, 30, and 580 mm, respectively, as shown in Fig. 3f. The sealing process was consistent with the site conditions, and the sealing was made by mixing cement, river sand, and water.

2.2.3.3 Pumping Flow Based on the geometric similarity conditions, the ratio of the geometric scale of the prototype to that of the model is defined as the reduction ratio α_1 . To eliminate the size effect of the coal body damage and instability, it is theoretically necessary to make the number and distribution of discontinuous surfaces in the model the same as those of the prototype. The ratio of the hole and crack feature size of the prototype to that of the model is also α_1 .

Based on the on-site hydraulic fracturing process design, the fracture hole diameter was 105 mm, the hole depth was 60 m, the pump flow rate was 200 L/min, and the pump pressure was 31.5 MPa. In the similar simulation experiment design, the hydraulic fracturing experiment has a water injection port diameter of 20 mm and a hole depth of 600 mm. According to the principle of geometric similarity:

$$\alpha_1 = l_p / l_m \quad (1)$$

Table 6 Stress sensor parameters

Name	Range	Frequency	Size	Number
CYY9 Soil stress sensor	0–30 MPa	0–1000 Hz	$\Phi 20 \times 8$ mm	6

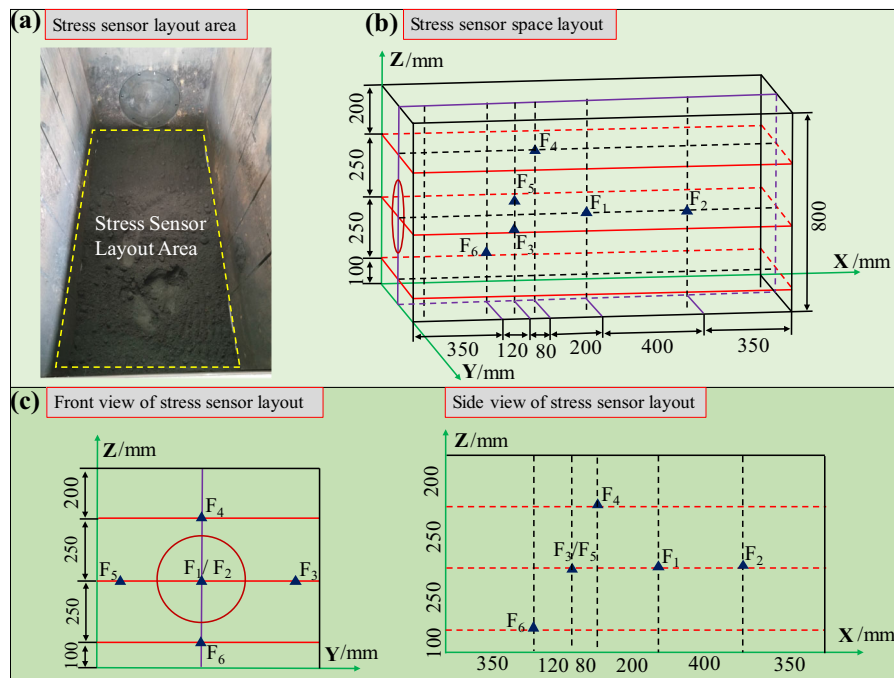


Fig. 4 Stress sensor placement system

The similarity ratio was calculated to be 690. The pump flow rate for calculating the hydraulic fracturing was 0.25 L/min. Based on the ground stress conditions, fracture hole parameters, and coal sample strength, the cracking pressure of the coal sample was approximately 6.4 MPa. Based on the ground stress conditions, parameters of the fracture holes and coal sample strength, the water injection capacity for the hydraulic fracturing was approximately 79.3 L.

2.2.4 Experiment Procedure

In the test, clear water was used as the fracturing fluid, which has advantages such as low compressibility and stable properties under high pressures. A large-scale geotechnical servo loading system, a hydraulic fracturing pump pressure servo control system, and an acoustic emission 3D positioning monitoring system were also employed together. The specific steps are as follows:

- (1) The 800 mm × 800 mm × 1500 mm sample was pressed in the fracturing cavity, and the stress sensor was layered in the process of pressing to

test the change law of the coal seam stress during hydraulic fracturing.

- (2) With construction fracturing drilling and acoustic emission drilling, 4 acoustic emission monitoring holes were drilled around the fracturing hole of the fracturing sample, and two acoustic emission probes were placed. The acoustic emission probe was bonded to the steel pipe using a coupling agent.
- (3) The hydraulic fracturing pump pressure servo control system and the acoustic emission monitoring system were started after loading the sample. A physical model testing machine was used to complete the vertical and horizontal stress loading. During the loading process, the axial and lateral pressures were alternately applied, with a pressure of 2 MPa. The axial pressure was 12 MPa, and the lateral load was 10 MPa, keeping it consistent with the on-site stress conditions. After the stress loading was completed, the servo system stabilized and maintained the pressure of the control system. The pump pressure displacement was used as the control mode to inject the fracturing fluid into the sample, and the computer

synchronously collected real-time acoustic emission and stress data of the pump injection pressure during the hydraulic fracturing process.

- (4) After the sample fracture channel was completely penetrated, the hydraulic fracturing pump pressure servo control system was switched off. After the pump pressure gradually decreased to a stable value, the data collection, acoustic emission, and stress information monitoring were stopped, and finally, the physical model tester was smoothly unloaded to 0.
- (5) Through a comprehensive analysis of the hydraulic fracturing pump pressure–time curve, acoustic emission monitoring information, and crack extension information described by the red tracer in the sample, the cracking and expansion rules of the hydraulic cracks and the spatial distribution pattern were analyzed after fracturing. The formation mechanism of the network fractures in the hydraulic fracturing of the coal and rock reservoirs is discussed preliminarily.

3 Results and Discussion

3.1 Distribution of Primary Cracks in Coal Samples

The original fracture distribution test was carried out during the construction of the hydraulic fracturing hole and the acoustic emission monitoring hole, as shown in Fig. 5a. The hydraulic fracturing hole is the No. 1 hole, the diameter and length of which are 0.60 m and 0.70 m, respectively; the remaining holes are acoustic emission test holes. For holes 2–5, the hole diameter is 0.30 m, and the length is as shown in Fig. 5a. During the construction drilling process, the coal sample was marked with crack marks, as shown in Fig. 5c. The number of fractures was detected, and the original fracture distribution of the coal sample was obtained on the basis of its position in the borehole, as shown in Fig. 5b. Fig. 5b shows that there are many primary cracks distributed in the coal sample near drilling holes 1–3, and the hydraulic fracturing process is prone to cracking, and the crack is easy to extend in this direction. To avoid new cracks due to the rig disturbance during the drilling process, the

corresponding drill pipe was equipped, the drilling rig was fixed during the drilling process, and no drill pipe transfer was required during the drilling process.

After the hydraulic fracturing was completed, the collected stress sensor data were analyzed. Two unmeasured sets of data from the six stress sensors arranged before the fracturing were noted. Therefore, the stress data reported in this paper come from the F1–F4 stress sensors.

3.2 Stress and Acoustic Emission Response During Confining Pressure Loading

Figure 6 shows the stress change and acoustic emission response during the confining pressure loading process.

Figure 6 shows that the acoustic emission and stress vary during the confining pressure loading process, and there is also a certain relationship between the two. Acoustic emission events can be measured throughout the confining pressure loading process, indicating that energy is released throughout this process. In the 25–45 s interval, the most common acoustic emission events occur, up to 400, mainly due to the deformation and stress redistribution of the surrounding coal body around the stress sensor. During the confining pressure loading process, the stress acting on the coal sample is mainly compressive, and the confining pressure is continuously loaded. The stress is transmitted through the coal body around the sensor, and the original state of the coal sample particles changes. The energy accumulated by the confining pressure begins to be released in large quantities. As the loading continues, the coal around the stress sensor reaches a rebalancing state, and the acoustic emission event no longer increases. During the confining pressure loading process, the stress gradually increases, whereas the stress changes monitored by the stress sensors at different positions are different. This is because the distributions of the primary cracks and coal particles near the stress sensors at different positions are not the same, resulting in the attenuation of the stress during the transfer. The magnitude is different. The F4 response is the strongest, with the maximum reaching 10 MPa, F1 and F2 responses are second, and the F3 response is the weakest. The stress decreases in the interval of 20–30 s, which may be due to the loosening of the surrounding coal body during the process of

Fig. 5 Distribution of primary cracks in the coal samples

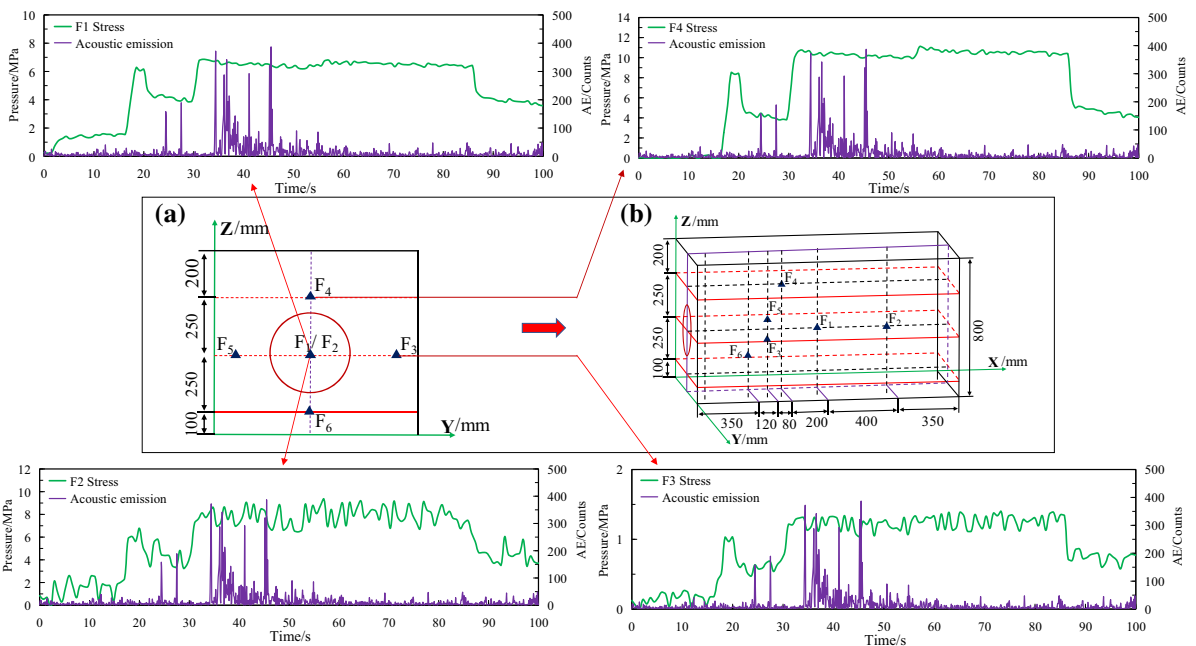
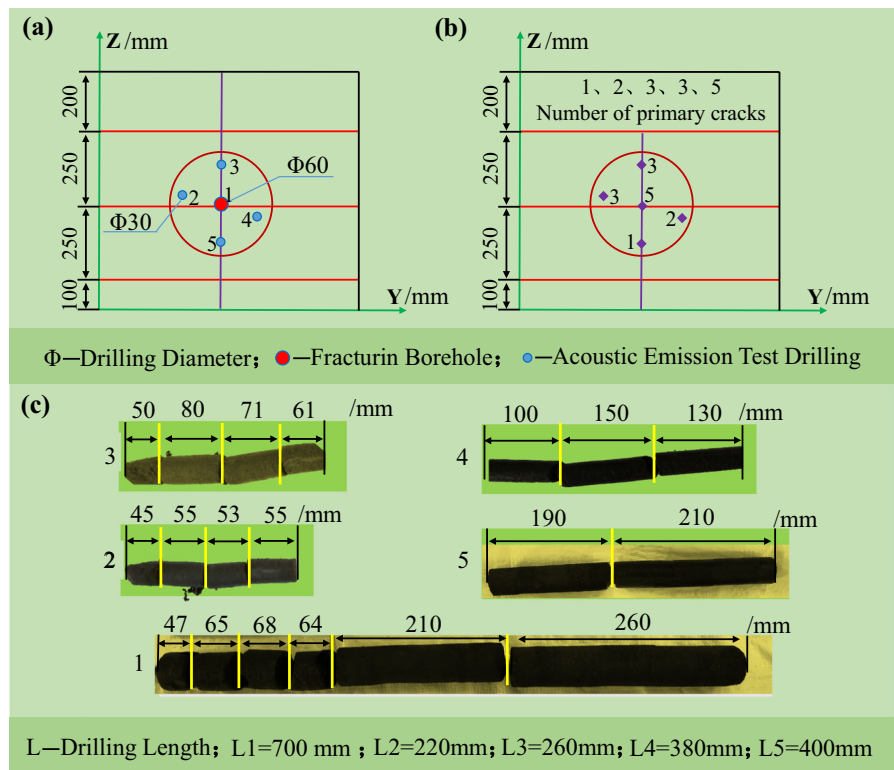


Fig. 6 Stress change and acoustic emission response during confining pressure loading

constructing the fracture hole and embedding the sensor. As the confining pressure increases, a part of

the pressure after the stress reaches the strength of the coal body is mainly used to compact the coal body.

The above data show that the coal sample is mainly subjected to compressive stress during the confining pressure loading process and that the compressive stress is transmitted by the coal sample as the medium, which is affected by factors such as the original crack and coal sample density.

3.3 Stress and Acoustic Emission Response During Hydraulic Fracturing

The stress change during hydraulic fracturing is the core indicator of the response to hydraulic fracturing. The stress sensor was used to test the stress change during hydraulic fracturing, and the stress response during hydraulic fracturing was explored, as shown in Fig. 7.

The hydraulic fracturing section can be divided into three stages depending on the water injection pressure. The first stage is the primary fracture filling and expansion stage. The figure shows that the four sensor stresses increase at this stage, because of the pressure water immersed in the coal seam during the hydraulic fracturing process. The magnitude of the stress increase is different: F4 has the greatest increase,

followed by F1 and F2, and the least is F3. Figure 7 shows that the primary fissure development area is prone to new fissures and that the fissures are more easily extended. This is because hydraulic fracturing is the support of the weak wall by the fluid water in the weak faces of the coal seam. The fractures open, expand, and extend to form an internal division of the coal seam. Due to the existence of the pore-fracture system of the coal body and the spatial positional relationship between the plane where they are located and the direction of the principal stress in the stress field of the original rock, there is a difference in the order of water intrusion into the coal body and its motion state. The rupture pressure in the first stage increases because the rupture sequence of the coal body during the hydraulic fracturing process begins with a large crack with a large opening degree and weak coupling ability; this is followed by a secondary crack and eventually a primary microcrack. The concentrated area where the acoustic emission count occurs is the first stage of hydraulic fracturing.

The second stage is the main crack initiation and expansion stage. At this stage, the pressure water is continuously immersed in the coal seam. The main

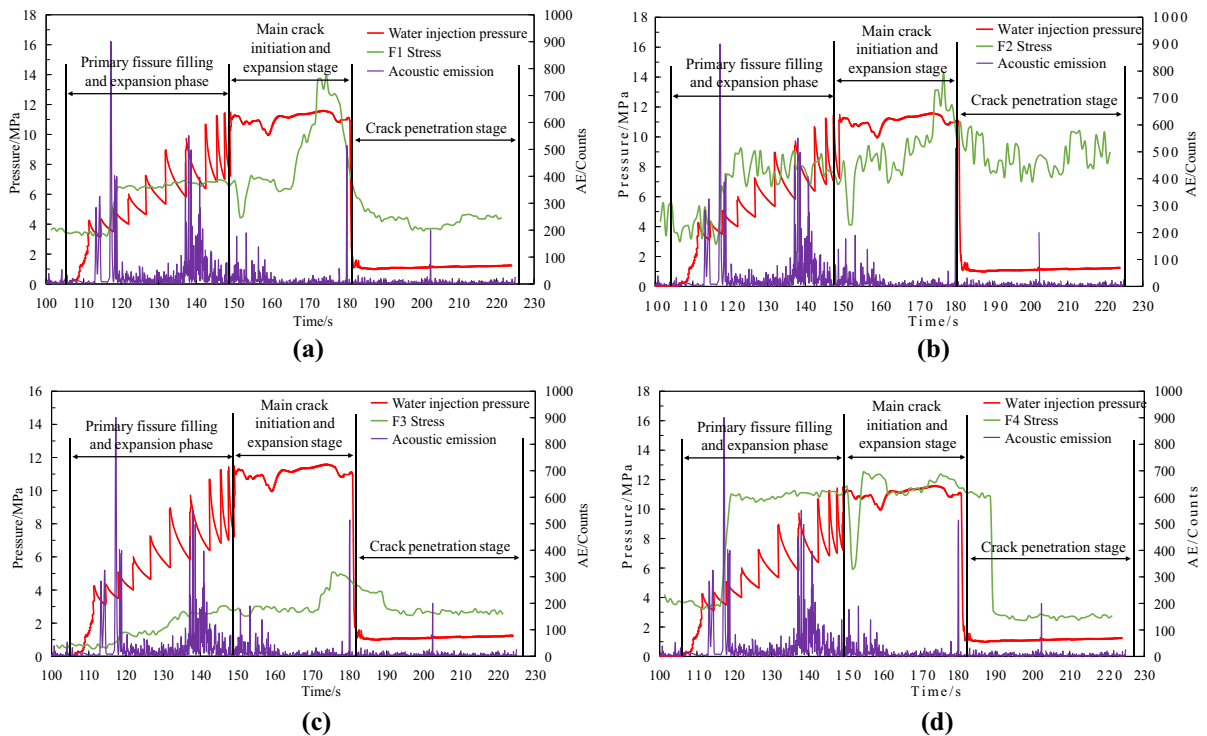


Fig. 7 Stress and acoustic emission changes during hydraulic fracturing

function of the pressure water is to fill the crack space that has been generated. Few parts act on the creation of new fissures; hence, there is no large accumulation of acoustic emission counts. Due to the extension of the primary fracture in the first stage, the main fracture cracks and expands at this time, and the pressure water directly acts on the stress sensor, thereby significantly increasing the stress.

The third stage is the fracture-through stage. At the time when the stress in the third stage begins to decrease, the acoustic emission has a large count accumulation, which is due to the continuous injection of the pressurized water at this time, which penetrates the crack in the coal sample. When the pressure water load continues to act on the coal body, a high-stress concentration occurs at the internal crack tip. When the stress exceeds the strength of the coal sample body, the internal crack of the coal sample penetrates completely, forming a more complex fracture network. Continued water injection pressure no longer increases, the injected pressure water emerges from the cavity, and the stress also drops sharply. The large-scale effluent area of hydraulic fracturing is also the original fissure development area, indicating that the fissures in the hydraulic fracturing process are more likely to extend to the original fissure development stage.

4 Spatiotemporal Evolution Mechanism of Coal Seam Stress

4.1 Coal Seam Stress and Crack Propagation

Figure 7 shows a sample stress curve and acoustic emission count diagram. First, after the hydraulic fracturing starts, the fracturing fluid gradually fills the fracturing cavity, and the pump pressure continues to rise, and this stage remains for approximately 15 s. The number of acoustic emissions produced in each area of the specimen is different.

As the fracturing fluid is continuously immersed in the coal seam, the pump pressure maintains a non-fixed and periodic increase, characterized by ascending and descending stages. As the fracturing fluid is continuously injected, the pressure increases to the fracture condition, the fracture expands, the accumulated water pressure decreases, and the crack temporarily stops expanding. Subsequently, the water

continues to fill, the water pressure increases again to the fracture condition, and the crack continues to expand. At this stage, the pressure continuously repeats the process of “filling water-boosting-releasing pressure.” At the moment of pressure relief, the crack spreads forward once, and the acoustic emission signal appears once, which maintains the same pace with the change in the pump pressure curve. The stress change measured by the stress sensor in different directions is different, and the stress increase near the outer wall of the coal sample is high. In addition to a part of the fracturing fluid directly acting on the squeeze stress sensor of the coal seam, it may also be because the outer wall of the sample is a rigid structure without deformation, and a part of the transmitted force will be reversely transmitted. At this time, the stress measured by the stress sensor is the stress overlay value. When the pressure reaches the rupture condition, the sample is penetrated, and the pump pressure and coal seam stress drop sharply.

Acoustic emission counts reflect the change in the cracks to a certain extent, and the number of dense acoustic emissions is generated at the moment when the pump pressure and coal bed stress decrease. The above results show that the emergence of acoustic emission signals is accompanied by the transmission of coal seam stress. Exploring the stress evolution mechanism of coal seam hydraulic fracturing has become the basis for studying the stress changes and crack extension laws.

4.2 Space–Time Effect of Coal Seam Stress Transmission

The stresses of the coal samples during confining pressure loading and hydraulic fracturing increase to different extents. To explore the stress change and transmission law of the coal seam more effectively, this study takes the stress increase index as the reference, and the interval is 10 s. Nodes extract the real-time stress data for the analysis.

The formula for the stress increase index is:

$$\delta = \frac{F_s - F_{\min}}{F_{\max} - F_{\min}} \quad (2)$$

where δ is the stress increase index, F_s is the real-time stress value, F_{\max} is the maximum stress during the hydraulic fracturing process, and F_{\min} is the minimum stress.

The water pressure value P and the coal layer stress values F1-F4 in the fracturing process are substituted into Eq. (2) to obtain the corresponding stress increase index. Subsequently, the surfer software is used to present the stress increase index, as shown in Fig. 8.

Figure 8 shows that the F2 stress change is the smallest in the hydraulic fracturing process, F3 is the second, and F1 and F4 are the highest, which is due to the different primary crack distributions in the coal samples. The primary fissures at F1 and F4 develop, and the fissures are more likely to extend to the primary fissure development zone during hydraulic fracturing. In Fig. 12a–d, the increase trend in the water injection pressure is the same as that of F1, indicating that the pressure water 30 s before hydraulic fracturing mainly extends the crack near F1. The pressurized water acts on the coal near F1, and the coal body creates new cracks, which produce a tip effect in front of the crack extension. At this time, the coal body damage region increases the stress by acting on the stress sensor. Different from the surrounding rock loading, the shear stress generated by the pressure-water expansion crack is the main force in the hydraulic fracturing process.

Under complex formation conditions, the pore wall of the coal rock fracturing pores undergoes shear failure in a three-way compression under hydraulic fracturing conditions. The common shear failure criterion is mainly the Mohr-Coulomb criterion. The criterion states that the material failure morphology and the magnitude of the shear stress on the failure

surface depend on the normal stress on the surface. In the compression zone, the material is a shear failure mode under normal stress, that is, compression shear failure, and the shear stress is also proportional to the normal stress of the surface.

The original ground stress and the mechanical properties of the coal play an important role in the process of hydraulic fracture propagation, which determines the shape of the coal body. The extended orientation of the hydraulic crack depends on the orientation and relative size of the three-way principal stress. Assuming that the coal body is an isotropic body, the wall of the borehole may be subjected to high-stress shearing under the action of a three-direction unequal pressure. The pressurized water then enters the shear rupture surface to promote crack opening and expansion. In this process, the tensile strength of the coal rock is the main factor. At this time, the tensile failure mode may be dominant. The expansion path of the crack is selected according to the principle of minimum energy. At the same time, in the process of crack flow expansion, the pressure on the crack surface and the three-direction stress difference will also cause shear failure to form a shear crack surface, and then, the pressure water begins to stretch and break on the crack surface. The crack is extended in the process of shear-stretching or stretching-shearing. Regardless of the shear rupture surface, the crack will be deflected during its extended extension and eventually becomes orthogonal to the direction of the minimum principal stress. Therefore, it can be

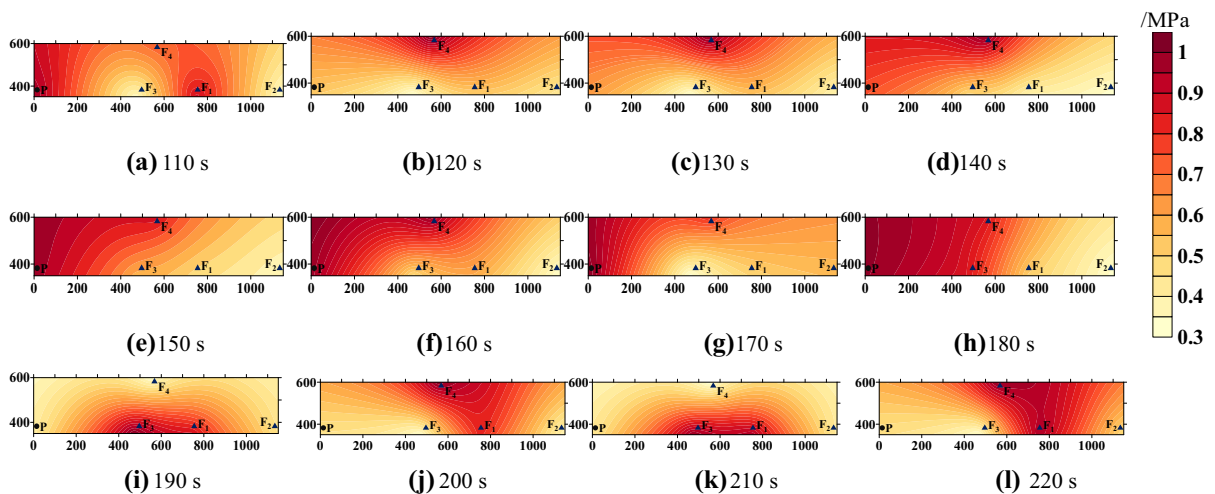


Fig. 8 Stress increase index during hydraulic fracturing (P-water injection pressure; F1, F2, F3, F4 - coal seam stresses)

considered that once the normal stress on the shear fracture surface is equal to zero, the crack begins to expand.

As the fracturing continues, the water injection pressure gradually increases, as shown in Fig. 8e–h. As the water injection pressure increases, the F4 stress gradually increases, and this corresponds to the second stage of hydraulic fracturing. The continuous injection of the pressure water causes the internal energy of the coal sample to accumulate continuously. When the energy accumulated inside the coal sample exceeds the energy required for the coal sample to crack, a new crack is generated, and the coal sample crack is completely penetrated. During the macroscopic cracking of the coal sample, the accumulated energy is continuously released, and this stage is also the most frequent phase of the acoustic emission test event. After the coal sample is completely fractured, the water injection pressure drops sharply, and the coal seam stress gradually decreases, as shown in Fig. 8i–l. At this stage, the stress gradually decreases. The pressure water mainly flows out through the cracks of the coal that has completely fractured. The coal sample stress is drastically reduced because the force of the water injection pressure acting on the coal sample is insufficient to cause stress transfer in the coal rock medium. In the process of stress transmission, it is affected by various factors, such as primary crack and coal sample density, and the crack is the major obstacle affecting stress transmission. With the continuous generation of new fissures in the hydraulic process, the effect of stress transfer on coal-like media is worsened. In the process of on-site hydraulic fracturing, the variation law of the stress can be used to explore the variation in the distribution area of the fracture during hydraulic fracturing, providing a new idea for exploring the expansion and extension of fractures during hydraulic fracturing.

This is different from the compressive stress of the coal seam during confining pressure loading. The stress of the coal seam during hydraulic fracturing is mainly shear stress. Both can be transmitted through the coal samples. With the continuous expansion and extension of the cracks during hydraulic fracturing, the stress transfer effect becomes increasingly weaker.

The stress transfer mode and size of the coal samples at different time points in the hydraulic fracturing stage are different. The loading process is mainly based on compressive stress, whereas the shear

stress is the dominant factor during the fracturing process. This is the time for stress evolution effect. As the hydraulic fracturing experiment is carried out, the stress attenuates to varying degrees with the change in the distance during the coal sample transfer process, which is determined by the spatial effect of coal seam hydraulic fracturing stress evolution.

5 Conclusion

Coal seam stress changes continuously with hydraulic fracturing. In this study, a large-scale physical similarity simulation test was designed in a laboratory. The surrounding rock stress sensor and acoustic emission were used to monitor the stress changes during hydraulic fracturing, and the stress variation law and crack extension law during hydraulic fracturing were explored. Based on the theory of damage mechanics, the law of coal-like fissure extension in the hydraulic fracturing process was explored. The following conclusions can be drawn from the research:

- (1) During the hydraulic fracturing process, the new fissures are more likely to extend to the primary fissure development zone. When the applied coal body stress exceeds the strength of the coal sample body, the internal crack of the coal sample is completely penetrated. As the accumulated energy of the pressurized water is continuously released, the count detected by the acoustic emission increases sharply.
- (2) The coal body is mainly subjected to compressive stress during the confining pressure loading process. During the hydraulic fracturing process, the coal body is mainly subjected to a shear stress, and both can be transferred through the coal sample. When the stress increase during hydraulic fracturing is greater than the confining load, the effect is due to different stresses.
- (3) The compressive stress is transmitted by the coal sample as the medium, and the transfer process is affected by factors such as the original crack and the density of the coal sample. As the cracks continue to expand and extend during hydraulic fracturing, the stress transfer effect becomes weaker. Through the large-scale hydraulic fracturing physical simulation test in the laboratory, it is feasible and effective to use

the simulated site conditions to determine the stress transfer law during the hydraulic fracturing process, providing a scientific guidance for the on-site hydraulic fracturing process.

Acknowledgments This work was financially supported by the Basic and Frontier Research Project of Chongqing (Grant No. cstc2020jcyj-bsh0132), the National Science and Technology Major Project of China (Grant No. 2016ZX05043005), the National Natural Science Foundation of China (Grant No. 51604045).

References

- Abass H H (1990) Experimental observations of hydraulic fracture propagation through coal blocks. *SPE* 21289.
- Abass H H (1991) Mathematical and experimental simulation of hydraulic fracturing in shallow coal seams. *SPE* 23452.
- Dahi-Taleghani Arash, Olson Jon E (2009) Numerical modeling of multi stranded hydraulic fracture propagation: accounting for the interaction between induced and natural fractures. *SPE* 124884:1150
- Bell G J, Jones A H (1989) Coal seam hydraulic fracture propagation on a laboratory scale. *Proceedings of the 1989 Coal-Bed Methane Symposium*.
- Chen M, Pang F, Jin Y (2000) Experiments and analysis on hydraulic fracturing by a large-size triaxial simulator. *Chin J Rock Mech Eng* 19(S1):868–872
- Dehghan AN, Goshtasbi K, Ahangari K (2016) Mechanism of fracture initiation and propagation using a tri-axial hydraulic fracturing test system in naturally fractured reservoirs. *Eur J Environ Civil Eng* 20(5):560–585
- Deng GZ, Wang SB, Huang BX (2004) Research on behavior character of fracture development induced by hydraulic fracturing in coal-rock mass. *Chin J Rock Mech Eng* 23(20):3489–3493
- Jin ZM, Song XM, Xue YD (1999) Test study of the top coal fracture. *J China Coal Soc* 24(2):180–182
- Khodaverdian M, McLennan J, Jones A H, et al (1991) Influence of near wellbore effects on treatment pressure in coal. *Proceedings of the 1991 Coal-Bed Methane symposium*. 1991.
- Li QS, Xing HL (2015) Numerical analysis of the material parameter effects on the initiation of hydraulic fracture in a near wellbore region. *J Nat Gas Sci Eng* 27:1597–1608
- Lin HX, Du CZ (2011) Experimental research on the quasi threeaxis hydraulic fracturing of coal. *J China Coal Soc* 36(11):1801–1805
- Meng SZ, Hou B, Zhang J (2016) Experimental research on hydraulic fracture propagation through mixed layers of shale, tight and coal seam. *J China Coal Soc* 41(1):221–227
- Papadopoulos J M, Narendran V M, Cleary M P (1983) Laboratory simulation of hydraulic fracturing. *SPE Symp Low Permeability* :161-174.
- Shi XY, Wen GJ, Bai JH (2016) A physical simulation experiment on fracture propagation of coal petrography in hydraulic fracturing. *J China Coal Soc* 41(5):1145–1151
- Shi MY, Jin Y, Chen M (2008) A physical simulation experiment study on hydraulic fracture extension in the horizontal well. *J Oil Gas Technol* 30(3):130–133
- Teufel LW, Clark JA (1984) Hydraulic fracture propagation in layered rock: experimental studies of fracture containment. *Soc Pet Eng J* 24(1):19–32
- Wong R. H. C., Wang S. W (2002) Experiment and numerical study on the effect of material property, normal stress and the position of joint on the progressive failure under direct shear. *mining and tunneling innovation and opportunity*. Toronto :1009-1016.
- Wang GQ, Xie XH, Su BY (2006) Experimental study of hydraulic fracturing of rock mass. *J Min Saf Eng* 23(4):480–484
- Zhou J, Chen M, Jin Y (2007) Experimental study on propagation mechanism of hydraulic fracture in naturally fractured reservoir. *Acta petrolei Sinica* 28(5):206–210

Publisher's Note Springer Nature remains neutral with regard to jurisdictional claims in published maps and institutional affiliations.